ORIGINAL ARTICLE

Neutrophil-modulated Dicer expression in macrophages influences inflammation resolution

Zhishang Wang[1] · Wenhua Li[2] · Jia Li[3] · Tianrong Jin[4] · Hong Chen[5] · Feihong Liang[6] · Shengran Liu[2] · Jialin Jia[2] · Tingting Liu[2] · Yu Liu[2] · Liming Yu[1] · Xiaodong Xue[1] · Jikai Zhao[1] · Tao Huang[1] · Xinyi Huang[1] · Huishan Wang[1] · Yongsheng Li[7] · Bangwei Luo[2] · Zhiren Zhang[2]

Abstract

The precise molecular mechanisms through which neutrophils regulate macrophages in the progression and resolution of acute inflammation remain poorly understood. Here, we present new findings on the role of Dicer in regulating macrophage phenotypic transitions essential for proper inflammatory progression and resolution, influenced by neutrophils. Using a zymosan A (Zym A)-induced self-limited mouse peritonitis model, we observed that Dicer expression in macrophages was significantly reduced by neutrophil-derived IFN-γ during the progression phase, but gradually returned to normal levels during the resolution phase following the engulfment of apoptotic neutrophils. Our study on macrophage-specific Dicer1-depletion (Dicer1-CKO) mice demonstrated that inflammation in these mice was more severe during the progression phase, characterized by increased pro-inflammatory cytokines and enhanced neutrophil trafficking. Additionally, resolution was impaired in Dicer1-CKO mice, leading to the accumulation of uncleared apoptotic neutrophils. Specifically, the absence of Dicer in macrophages resulted in M1 polarization and heightened bactericidal activity, facilitating the progression of acute inflammation. Conversely, inducing Dicer expression promoted macrophage transition to M2 polarization, enhancing apoptotic cell clearance and expediting the resolution of inflammation. Our findings suggest that Dicer plays a central role in regulating the progression and resolution of acute inflammation, with implications for the treatment of inflammatory diseases.

Keywords Macrophage polarization · Neutrophil · Dicer · IFN-γ · Inflammation resolution · Efferocytosis

Zhishang Wang, Wenhua Li and Jia Li contributed equally to this work.

✉ Huishan Wang
huishanw@126.com

✉ Yongsheng Li
lys@cqu.edu.cn

✉ Bangwei Luo
luo6341@tmmu.edu.cn

✉ Zhiren Zhang
zhangzhiren@tmmu.edu.cn

1 Department of Cardiovascular Surgery, General Hospital of Northern Theater Command, No.83, Wenhua Road, Shenhe District, Shenyang, Liaoning 110016, China

2 Institute of Immunology, Army Medical University, 30 Gaotanyan Main Street, Chongqing 400038, China

3 Department of Nephrology, Navy 971 Hospital, 22 Minjiang Road, Qingdao, Shandong 266000, China

4 Medical College of Chongqing University, Chongqing 400030, China

5 Department of Orthopedics, No. 903 Hospital of PLA Joint Logistic Support Force, 14 Lingyin Road, Lingyin Street, Xihu District, Hangzhou, Zhejiang 310000, China

6 Department of Medical Science, Shunde Polytechnic, Foshan, China

7 Department of Medical Oncology, Chongqing University Cancer Hospital, Chongqing 400030, China

Introduction

Inflammation is a crucial part of the innate immune response, playing a key role in fighting off invading microorganisms and aiding in tissue repair [1]. The two main phases of acute inflammation are the pro-inflammatory progression and the subsequent resolution [2]. A swift and robust pro-inflammatory response is vital for eliminating pathogens, while a sluggish response can hinder the body's ability to protect against infection and injury. Successful resolution of acute inflammation involves timely termination of the reaction, followed by tissue remodeling and restoration of balance, a phase known as resolution [3, 4]. Inadequate resolution can lead to chronic inflammation, excessive tissue damage, and impaired healing, resulting in fibrosis [5]. Neutrophils and macrophages are key players in regulating inflammation progression and resolution, with neutrophils playing a role in both pro-inflammatory and anti-inflammatory processes, crucial for resolution [6]. However, the mechanisms involved in transitioning from the pro-inflammatory phase to the anti-inflammatory resolution phase are not well understood.

Depending on the microenvironment, macrophages can acquire either the 'M1' or 'M2' phenotype, allowing them to exhibit pro-inflammatory or anti-inflammatory behavior, respectively [7]. M1 macrophages differentiate in response to bacterial moieties like LPS and IFN-γ, characterized by the expression of inducible nitric oxide synthase (iNOS) and the production of pro-inflammatory cytokines such as TNF-α and IL-6. On the other hand, M2 macrophages develop after exposure to IL-4, IL-10, and IL-13, displaying an anti-inflammatory phenotype with high expression of CD206, Arginase 1 (Arg1), and FIZZ1, along with increased release of anti-inflammatory cytokines like transforming growth factor (TGF)-β and IL-10, and reduced production of pro-inflammatory cytokines [8]. Recent research indicates that macrophages transition from the initial M1 activation in the progressive phase to a later M2 state in the resolution phase [9, 10]. In the progressive phase, M1 macrophages use pro-inflammatory molecules to recruit more neutrophils and monocytes to the site of inflammation, aiding in the host's defense against foreign pathogens. Conversely, during resolution, M2 macrophages have an anti-inflammatory role and are crucial for clearing apoptotic cells, leading to the production of specialized pro-resolving mediators (SPMs) and the active resolution of inflammation [11, 12]. Therefore, the polarization of macrophages is a critical regulatory mechanism that influences the progression and resolution of inflammation. Nonetheless, it remains uncertain whether any mediators promoting the progressive phase of inflammation can trigger a resolution program. Nevertheless, the interaction between neutrophils and macrophages is a crucial aspect of the inflammatory process [13]. Neutrophils release pro-inflammatory cytokines during the early stages of infection, inducing a M1 phenotype in macrophages to enhance microbicidal activity [14]. Conversely, IL-13 secreted by neutrophils can shift macrophage polarization to the M2 phenotype during helminth infections to combat parasitic worms effectively [15]. Additionally, the phagocytic clearance of apoptotic neutrophils can transform pro-inflammatory macrophages into an anti-inflammatory M2-like phenotype [16]. These findings demonstrate the diverse roles of neutrophils in modulating inflammation by regulating both M1 and M2 activation of macrophages as needed. However, the specific molecular mechanisms through which neutrophils orchestrate the transition of macrophages from M1 to M2 polarization remain largely unknown.

The regulatory network controlling macrophage polarization is complex, involving various factors including cytokines, metabolites like interleukin and Glutamine, and microRNAs (miRNA) as key regulators [17]. Dicer, responsible for processing miRNAs, plays a crucial role in this process [18]. Studies have shown that inhibiting Dicer activity or deleting Dicer enhances pro-inflammatory responses in macrophages and induces a M1-like programming in tumor-associated macrophages (TAM) [19, 20]. Conversely, Dicer has also been linked to anti-inflammatory effects in macrophages, such as inducing these effects with metformin through microRNA-34a-5p and microRNA-125b-5p [21]. These findings underscore the significance of Dicer in regulating macrophage M1/M2 polarization, although its exact role in the progression and resolution of inflammation remains incompletely understood. We suggest that Dicer plays a crucial role in both promoting and resolving acute inflammation processes.

In this study, we utilized Zym A-induced peritonitis in mice to investigate the progression and resolution phases of inflammation [22]. Our analysis focused on the expression profiles of Dicer in macrophages throughout the inflammatory process. Our results demonstrated that Dicer expression in macrophages is initially reduced by neutrophil-derived IFN-γ during the progressive stage of inflammation, but gradually increases as a result of engulfing apoptotic neutrophils in the resolution phase. This dynamic regulation of Dicer plays a crucial role in transitioning macrophages from a pro-inflammatory M1 state to an anti-inflammatory M2 phenotype. Interestingly, our findings suggest that macrophage-specific loss of Dicer impairs the clearance of apoptotic neutrophils, leading to delayed resolution of acute peritonitis in Dicer-CKO mice. Overall, our study uncovers a novel mechanism involving macrophage Dicer as a central regulator of inflammation progression and resolution, modulated by neutrophils.

Results

Macrophage Dicer is temporally regulated during acute inflammation

To investigate the impact of Dicer on acute inflammation, we utilized a well-established model of self-limited inflammation induced by zymosan A (Zym A). We analyzed the cellular composition in peritoneal exudate at different time points during peritonitis using flow cytometry. Neutrophils and monocytes/macrophages comprised over 95% of the cells, with neutrophils peaking at 6 h and gradually decreasing, while monocytes/macrophages continuously increased and became dominant at 48 h (Fig. 1A). Total cell count in the peritoneal exudate was documented over time (Fig. 1B). Line charts were generated based on the proportions of neutrophils and monocytes/macrophages, showing dynamic changes in cell count, including apoptotic neutrophils (Fig. 1A-D, Supplementary Fig. 1A-D). Inflammatory factors like TNF-α, IL-6, IL-10, IL-12p70, and MCP-1 peaked at 6 h and then decreased, while TGF-β, an anti-inflammatory factor linked to tissue repair, increased with inflammation progression (Fig. 1E, Supplementary Fig. 1E).
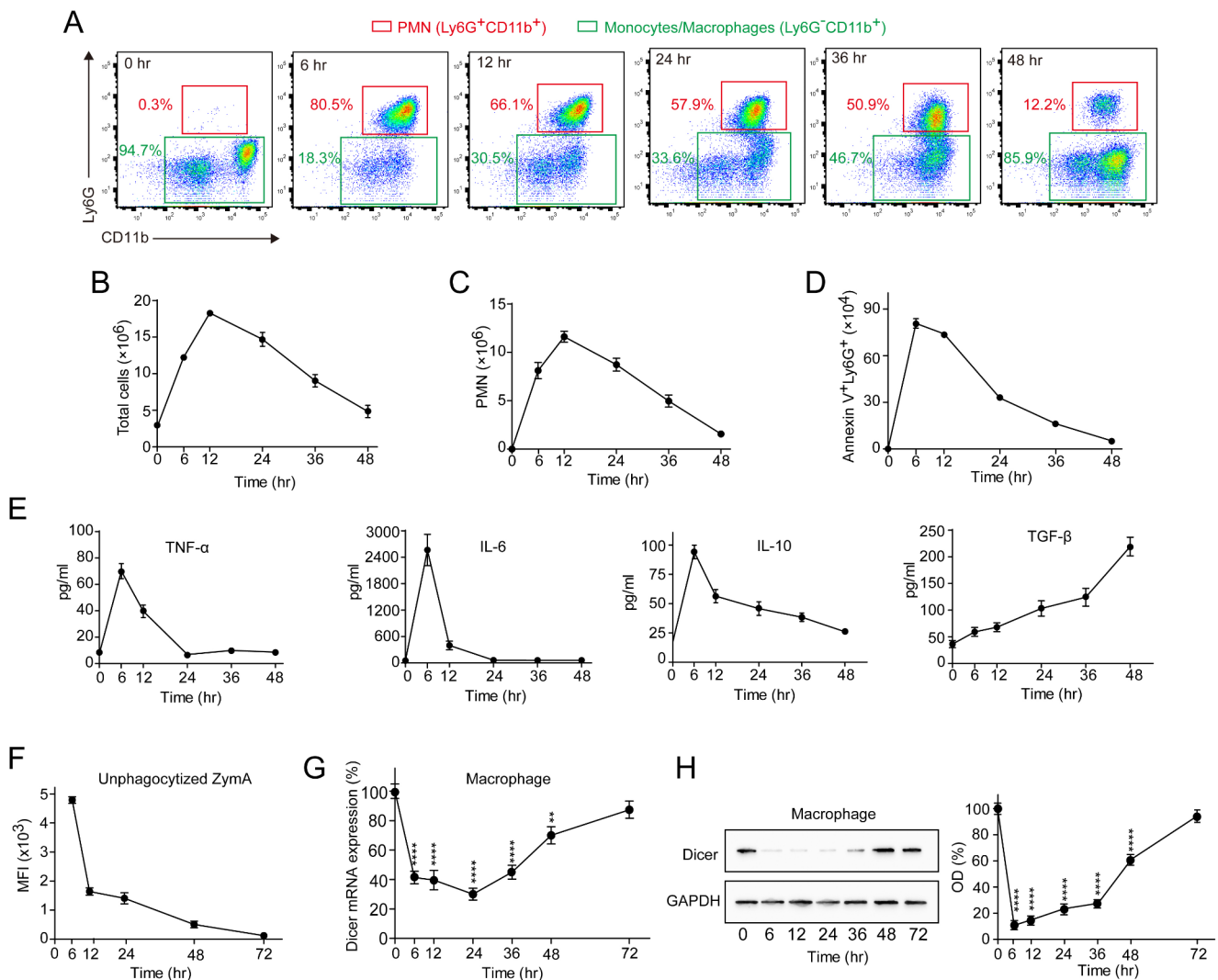

Fig. 1 Dicer is temporally regulated during inflammation resolution. WT mice were subjected to 1 mg Zym A for up to 48 h and peritoneal exudates were obtained at indicated intervals ($n = 6$ mice per group per time point). (**A**) The main cell populations (PMN, Ly6G$^+$CD11b$^+$ and monocytes/macrophages, Ly6G$^-$CD11b$^+$) in the peritoneal exudate during acute peritonitis were analyzed by flow cytometry. (**B-C**) Numbers of total cells (**B**) and neutrophils (**C**) in peritoneal exudate were enumerated. (**D**) Apoptotic neutrophils (Ly6G$^+$Annexin V$^+$) were analyzed by flow cytometry. (**E**) Protein concentrations of TNF-α, IL-6, IL-10 and TGF-β were assessed in exudates (0–48 h) by ELISA (pg/ml of total protein are shown). (**F**) The unphagocytized Zym A particles in peritoneal exudate analyzed by flow cytometry. (**G -H**) Dicer expression in macrophage during acute peritonitis analyzed by RT-qPCR (**G**) or western blot (**H**). Error bars represent SEM. Statistical analysis in Fig. 1G and H was performed *via* one-way *ANOVA* with Tukey's post-hoc test for multiple comparisons. *$p < 0.05$; **$p < 0.01$; ****$p < 0.0001$

These findings provide insights into the physiological state of acute inflammation.

In addition, we found that free Zym A in the peritoneal exudate was mostly cleared within 48 h (Fig. 1F). Flow cytometry analysis (Supplementary Fig. 1F) indicated that during peritonitis, over 80% of the free Zym A in the abdominal cavity was cleared by neutrophils and macrophages (Supplementary Fig. 1G-I). These findings suggest that in this model of acute inflammation, neutrophils and macrophages play a crucial role in controlling the progression and resolution of inflammation. To delve deeper into the regulatory mechanisms of acute inflammation, we examined the expression of Dicer in $Ly6G^-CD11b^+F4/80^+$ macrophages sorted by flow cytometry. The results revealed a decrease in Dicer expression during the inflammatory phase, which gradually recovered as inflammation resolved (Fig. 1G-H). The fluctuating levels of Dicer expression suggest its involvement in regulating acute inflammation.

Dicer deletion potentiates pro-inflammatory effect and leads to a delay in the resolution of peritonitis

To investigate the impact of macrophage Dicer on acute inflammation, we utilized LysM-Cre$^{+/+}$/Dicer1$^{loxp/loxp}$ (*Dicer1-CKO*) mice with macrophage Dicer knockout [23]. Our findings confirm that the deletion of Dicer in macrophages does not impact the development and maturation of monocytes/macrophages or other immune cells, such as neutrophils, T cells, and B cells in the spleen and bone marrow (Supplementary Fig. 2A-B). Additionally, no significant differences were observed in blood cells between wild-type (WT) and *Dicer1-CKO* mice (Supplementary Fig. 2C). The oxidative stress function, apoptosis, and mitochondrial function of polymorphonuclear leukocytes (PMNs) in the blood were also unaffected by Dicer knockout (Supplementary Fig. 2D).

In our study, we monitored the time points at which neutrophil numbers peaked (T_{max}) and decreased to half of the peak (T_{50}) following intraperitoneal injection of Zym A. The resolution interval of peritonitis (R_i) was determined by the difference between T_{max} and T_{50}. The time periods between 0 and 12 h and 24 to 48 h were designated as the initiation/progression and resolution phases of peritonitis, respectively. Our data showed that the peak of neutrophil count (ψ_{max}) in Dicer1-CKO mice was higher compared to Dicer1 control (*Dicer1-C*) mice, although the T_{max} values were similar. This discrepancy resulted in a 5-hour delay in R_i for the *Dicer1-CKO* mice (Fig. 2A).

To investigate the factors affecting the resolution of peritonitis, we analyzed the total cell count at 0, 6, and 12 h to track the progression of peritonitis. Our results showed that both the total cell count and neutrophil count in *Dicer1-CKO* mice were significantly higher compared to *Dicer1-C* mice, while the number of macrophages did not differ significantly between the two groups (Fig. 2B-D). Furthermore, levels of pro-inflammatory cytokines TNF-α and IL-6 exhibited a trend of increased secretion, while the anti-inflammatory cytokine IL-10 decreased at 12 h (Fig. 2E). Subsequent experiments involving the transfer of bone marrow derived macrophages (BMDM) from WT and *Dicer1-CKO* mice into the peritoneal cavity of *Dicer1-CKO* mice revealed that WT-BMDM led to reduced recruitment of neutrophils and lower levels of pro-inflammatory cytokines compared to KO-BMDM (Fig. 2F-J). This suggests that high Dicer expression in macrophages may play a role in limiting inflammation intensity during the progression phase of peritonitis.

The experiment was repeated in WT mice (Fig. 2K), showing that further reduction of Dicer expression (injection of KO-BMDM) led to a more robust development of peritonitis during the progression phase. This was attributed to an increased presence of inflammatory cells (Fig. 2L-N), up-regulated pro-inflammatory cytokines, and decreased levels of anti-inflammatory cytokines (Fig. 2O). These findings indicate that Dicer deletion has pro-inflammatory effects in the progression of inflammation. Additionally, an analysis of cells (Fig. 3A-C) and cytokines (Fig. 3D) from peritoneal exudate during the resolution of peritonitis at 24 and 48 h revealed that the delayed resolution of inflammation in *Dicer1-CKO* mice was due to excessive recruitment of neutrophils (Fig. 3B), hypersecretion of pro-inflammatory cytokines, and reduction of anti-inflammatory cytokines (Fig. 3D). Moreover, an increased number of apoptotic neutrophils in *Dicer1-CKO* mice during the resolution phase of peritonitis indicated impaired clearance of apoptotic neutrophils (Fig. 3E). In addition, Dicer deficiency induced impaired clearance of apoptotic cells was testified in another mouse skin wound-healing model as well, and TUNEL staining of the wound tissue revealed an increased accumulation of apoptotic cells in the *Dicer1-CKO* group (Fig. 3F). In this wound-healing model, we found that the wound healing process was significantly delayed in the *Dicer1-CKO* group (Supplementary Fig. 3A), with the *Dicer1-CKO* group exhibiting an R_i of 6.44, which was delayed by 4 days compared to the *Dicer1-C* group's R_i of 10.40 (Supplementary Fig. 3B). On Day 6, we measured the epithelial distance (d) between the two ends of the wound (Supplementary Fig. 3C) and found that the epithelial distance in the *Dicer1-CKO* group was substantially longer than that in the *Dicer1-C* group, while the granulation tissue area was notably smaller in the *Dicer1-CKO* group, suggesting a slower wound recovery rate in the *Dicer1-CKO* group. Overall, these results suggest that Dicer deletion may
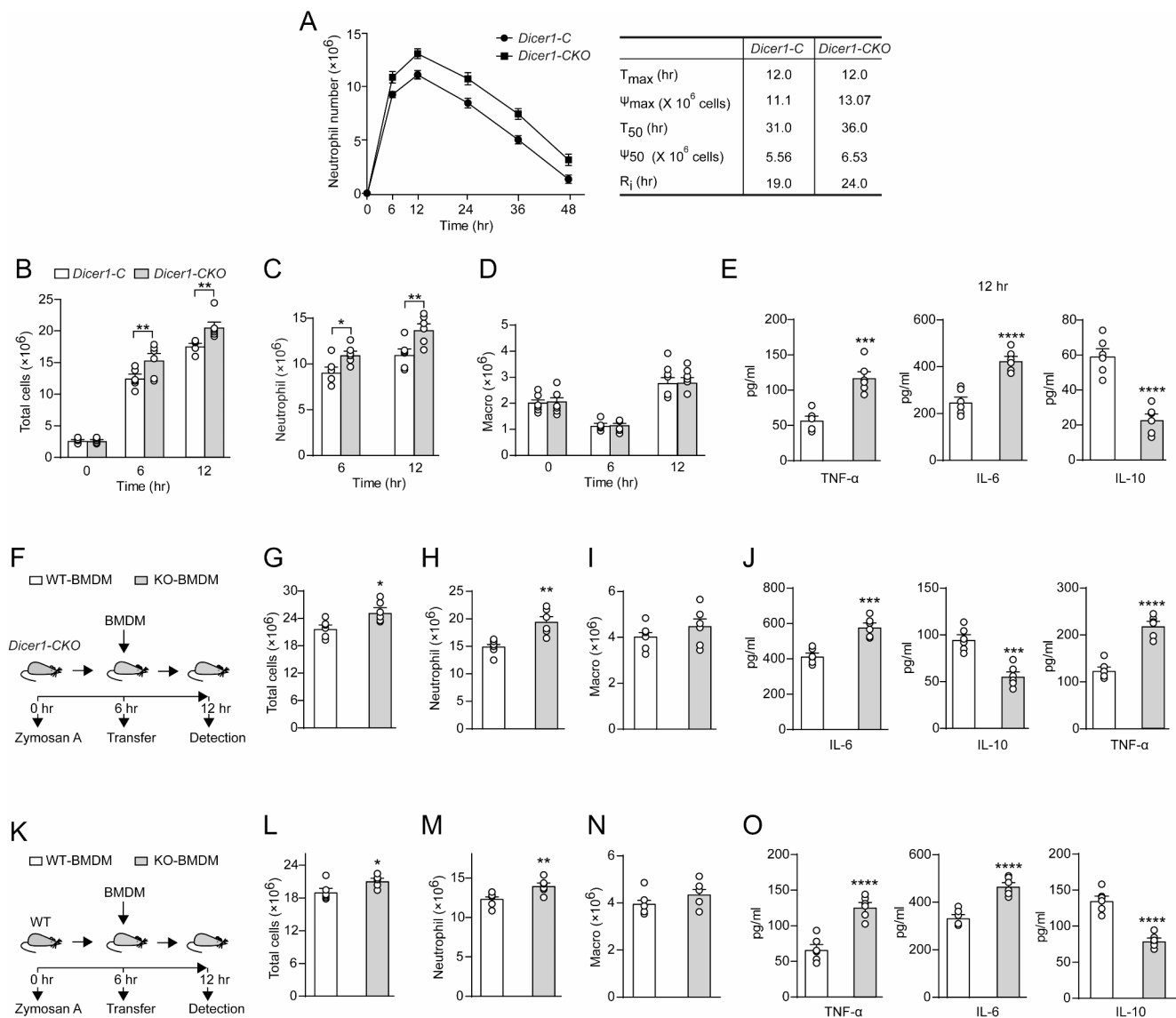
Fig. 2 Reduced Dicer expression promotes the progression of inflammation. (**A**) The resolution indices of *Dicer1-C* and *Dicer1-CKO* mice after Zym A-induced acute inflammation (*n*=6 mice per group). (**B-D**): Numbers of total cells (B, *n*=6), neutrophils (C, *n*=6) and macrophages (D, *n*=6) in peritoneal exudates were counted. (**E**) Inflammatory cytokines in cell-free peritoneal exudates at 12 h (*n*=6). (**F-J**) *Dicer1-CKO* mice were treated with WT-BMDM or KO-BMDM by intraperitoneal injection at 6 h after Zym A were given (**F**). The quantities of total cells (G, *n*=6), neutrophils (H, *n*=6), macrophages (I, *n*=6) and inflammatory cytokines (J, *n*=6) in peritoneal exudates were measured. (K-O) WT mice were treated with WT-BMDM or KO-BMDM by intraperitoneal injection at 6 h after Zym A were given (**K**). The quantities of total cells (L, *n*=6), neutrophils (M, *n*=6), macrophages (N, *n*=6) and inflammatory cytokines (O, *n*=6) in peritoneal exudates were measured. Error bars represent SEM. Statistical analysis in Fig. 2B, C and D was performed *via* two-way *ANOVA* with Tukey's post-hoc test for multiple comparisons, unpaired two-tailed Student's *t* test was used for the rest analysis. *p<0.05; **p<0.01; ***p<0.001

disrupt macrophage functions and contribute to a delay in the resolution of peritonitis.

Dicer deletion promotes macrophage polarization towards the M1 phenotype and strengthens their bactericidal ability

Macrophage polarization plays a crucial role in regulating the progression and resolution of acute inflammation. To analyze the mRNA expression pattern of macrophages, we conducted quantitative real-time PCR (RT-qPCR). Initially, we compared the phenotypic differences between macrophages isolated from *Dicer1-C* and *Dicer1-CKO* mice at 12 h post-peritonitis induction. Macrophages from *Dicer1-CKO* mice displayed a pro-inflammatory phenotype with elevated expression of M1 markers including *inos*, *tnfa*, *mcp1*, *il1b*, *il6*, and *il12p70* compared to *Dicer1-C* mice (Fig. 4A). Additionally, we used flow cytometry to confirm
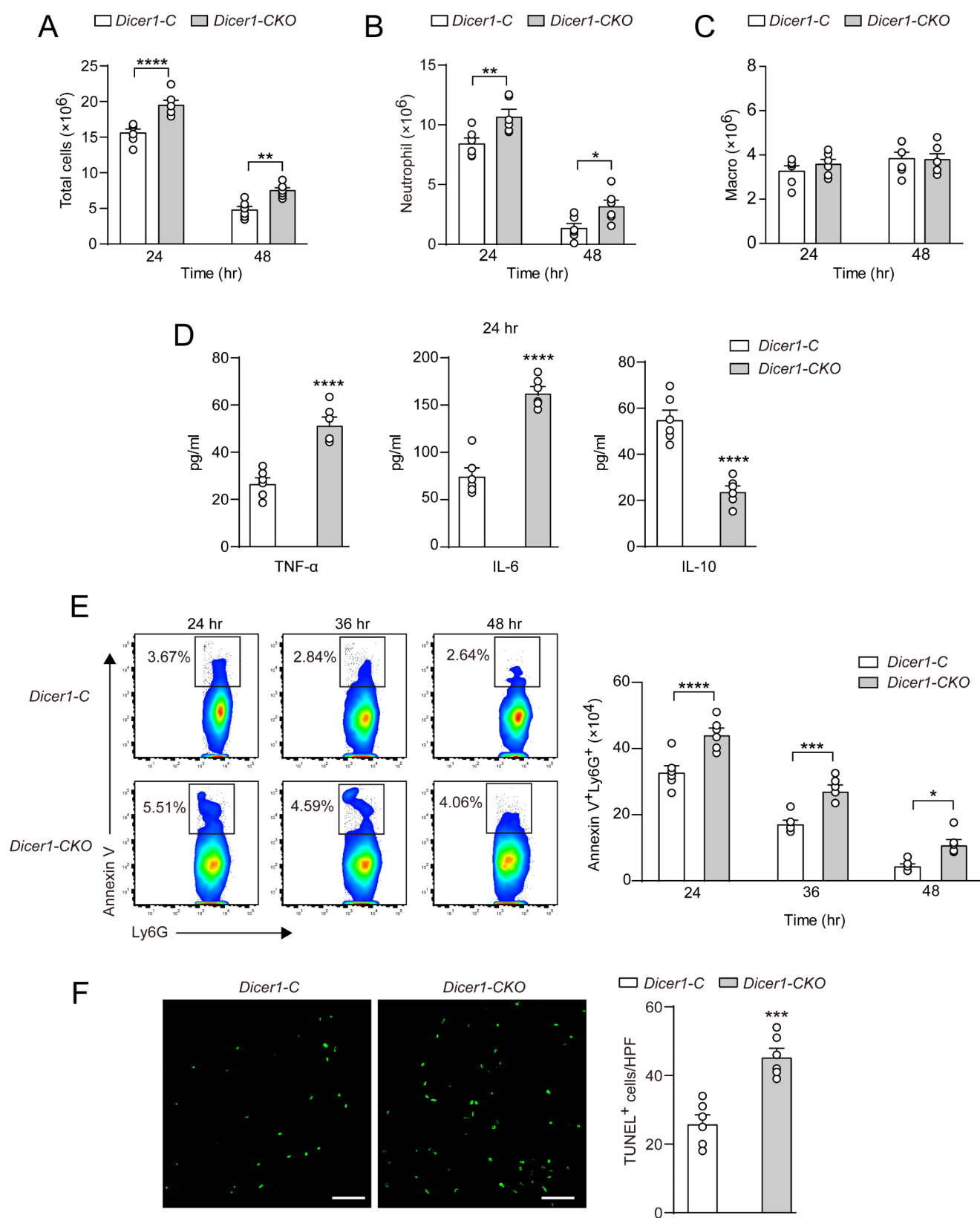
Fig. 3 Dicer deletion leads to a delayed resolution of peritonitis. *Dicer1-C* and *Dicer1-CKO* mice were intraperitoneally challenged with 1 mg Zym A to establish acute inflammation. Numbers of total cells (**A**), neutrophil cells (**B**) and macrophages (**C**) in peritoneal exudates were counted at 24 and 48 h ($n = 6$). (**D**) Protein concentrations of TNF-α, IL-6, IL-10 and TGF-β were assessed in peritoneal exudate (12 h) by ELISA ($n = 6$). (**E**) Apoptotic neutrophils (Ly6G$^+$Annexin V$^+$) were analyzed by flow cytometry ($n = 6$). (**F**) Full-thickness skin wounds of equal area were created in both *Dicer1-C* and *Dicer1-CKO* groups. Quantification of TUNEL$^+$ cells in wounds in 3–5 high-power fields (HPFs) per mice on day 6 ($n = 6$). Error bars represent SEM. Statistical analysis in Fig. 3D was performed via unpaired two-tailed Student's *t* test, two-way *ANOVA* with Tukey's post-hoc test for multiple comparisons was used for the rest comparison. *$p < 0.05$; **$p < 0.01$; ***$p < 0.001$; ****$p < 0.0001$

a significant increase in iNOS and TNF-α expression in macrophages from *Dicer1-CKO* mice in vivo (Fig. 4B-C). Furthermore, in vitro experiments showed that macrophages from *Dicer1-CKO* mice had increased dextran phagocytic capacity (Fig. 4D). These combined in vivo and in vitro results suggest that following Dicer depletion, macrophages tend to polarize towards an M1 phenotype, potentially enhancing their pro-inflammatory and antimicrobial functions.

To confirm the impact of Dicer deletion on M1 polarization and antimicrobial functions of macrophages, we generated a RAW264.7 murine macrophage cell line with suppressed Dicer gene expression using Dicer-siRNA. Following LPS stimulation, Dicer-siRNA treated macrophages exhibited significantly higher levels of *tnfa*, *il6*, and *inos* compared to the control group treated with scramble-siRNA (Supplementary Fig. 4A). Subsequently, we utilized a coculture system with bacteria such as *Staphylococcus aureus*, *Escherichia coli*, or *Listeria monocytogenes* along with Dicer-siRNA or scramble-siRNA treated RAW264.7 macrophages. Results indicated a marked decrease in colony forming units (CFU) of Dicer-siRNA macrophages, suggesting an enhanced bactericidal ability post Dicer-siRNA treatment (Fig. 4E). Furthermore, the expression levels of *tnfa*, *inos*, and *nox1* in Dicer-siRNA macrophages were notably higher when co-cultured with *L. monocytogenes*, underscoring the pro-inflammatory effects of Dicer deletion in promoting M1 macrophage polarization (Supplementary Fig. 4B). These findings collectively support the notion that Dicer deletion drives macrophage polarization towards the M1 phenotype and enhances pro-inflammatory responses.

Dicer deletion inhibits macrophage polarization towards the M2 phenotype and impairs macrophage efferocytosis

Dicer deletion has been shown to influence macrophage polarization towards the M1 phenotype. In this study, we investigated the impact of Dicer deletion on macrophage

M2 polarization. Using RT-qPCR analysis, we observed decreased expression levels of *arg1* and *fizz1*, markers of M2 macrophages, in KO-BMDM compared to WT-BMDM when induced by IL-4 (Fig. 5A). Furthermore, our findings revealed a significant reduction in the expression of *tgfb*, *arg1*, and *fizz1* in KO-BMDM compared to WT-BMDM when M2 polarization was induced by apoptotic thymocytes in vitro (Fig. 5B). Additionally, the expression of CD206 on peritoneal macrophages was notably lower in *Dicer1-CKO* mice compared to *Dicer1-C* mice, indicating impaired M2 polarization in the absence of Dicer (Supplementary Fig. 5A). Moreover, when M2 differentiation was induced in Dicer-deficient RAW264.7 cells using IL-4, a decrease in the expression of M2 polarization-associated molecules, including *arg1*, *fizz1*, and *pparg*, was observed (Fig. 5C). These results provide compelling evidence that Dicer deficiency hinders M2 polarization in macrophages.

M2 polarized macrophages have the ability to suppress excessive inflammatory responses and facilitate the resolution of inflammation by clearing apoptotic neutrophils. To assess the impact on the phagocytic function of macrophages, we conducted flow cytometry-based engulfment assays in vitro using apoptotic thymocytes labeled with CFSE. Our results, illustrated in Fig. 5D and Supplementary Fig. 5B, showed a significant reduction in the uptake of apoptotic thymocytes by *Dicer1-CKO* peritoneal macrophages. Additionally, we utilized Laser-scanning confocal microscopy to observe the engulfment of apoptotic thymocytes (Fig. 5E, Supplementary Fig. 5C), which consistently revealed impaired efferocytosis in *Dicer1-CKO* peritoneal macrophages. Subsequent flow cytometry assays conducted in vivo at 12, 24, 36, and 48 h demonstrated a more than 50% decrease in the percentage of engulfment by *Dicer1-CKO* peritoneal macrophages (Fig. 5F). In summary, the deletion of Dicer inhibits macrophage M2 polarization and negatively impacts macrophage efferocytosis, consequently leading to a delay in the resolution of peritonitis.

Neutrophil-derived IFN-γ and phagocytosis of apoptotic cells regulate Dicer expression in macrophages during peritonitis

The influence of Dicer on macrophages has been clarified, but the regulatory mechanism of Dicer expression in macrophages remains unknown. To investigate the dynamic changes in Dicer expression during different phases of peritonitis progression, we analyzed cytokines in the peritoneal exudate. Initially, we observed a negative correlation between IFN-γ expression levels (Fig. 6A) and Dicer levels (Fig. 1G, H). Subsequent flow cytometry analysis of IFN-γ receptor expression on neutrophils and macrophages in the peritoneal exudate at 24 h revealed that over 80%
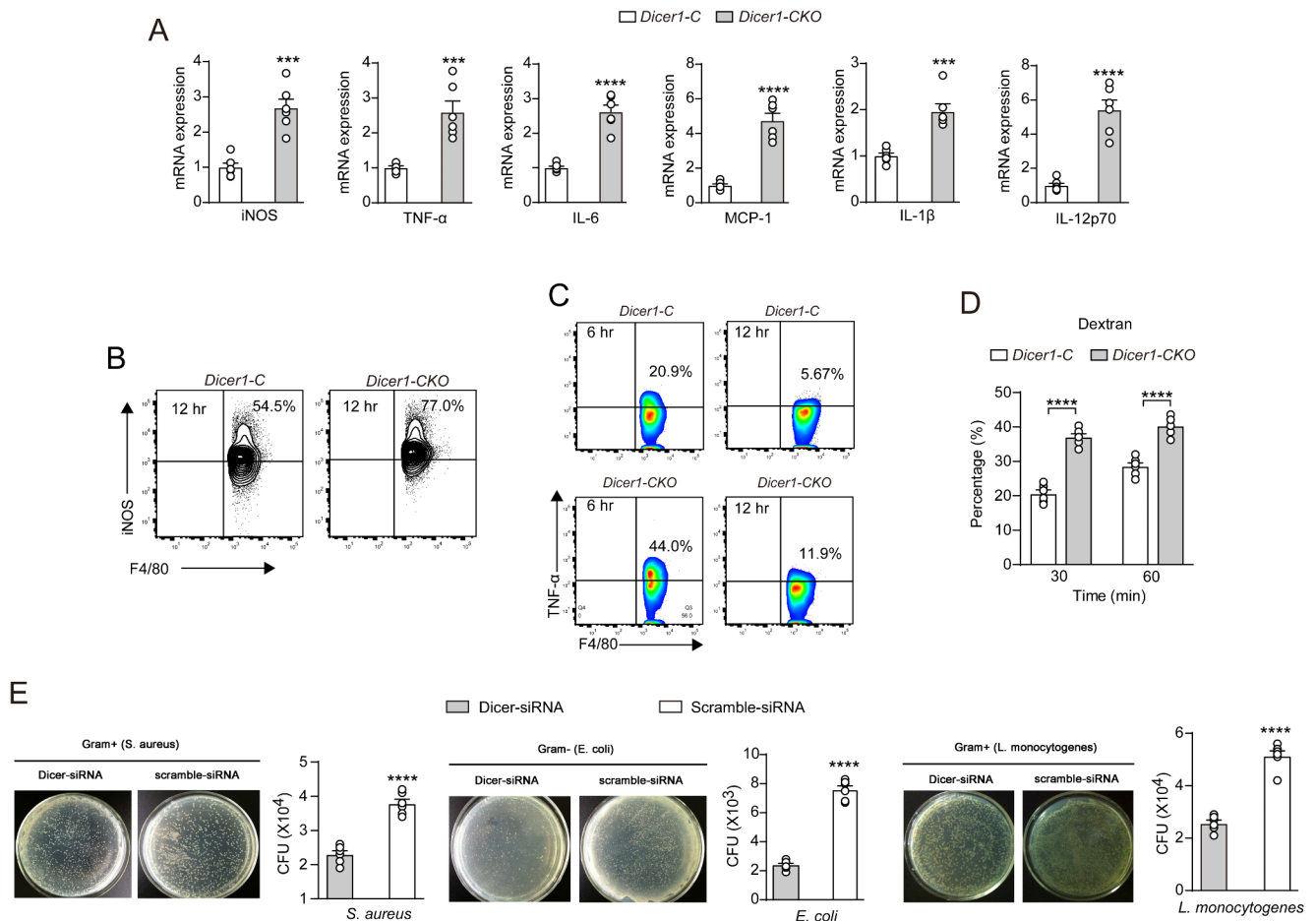
Fig. 4 Dicer deletion promotes macrophage polarization towards M1 phenotype. *Dicer1-C* and *Dicer1-CKO* mice were intraperitoneally injected with 1 mg Zym A to establish acute inflammation. (**A**) Macrophages were isolated from the peritoneal exudate at 12 h and mRNA expression of iNOS, TNF-α, MCP-1, IL-1β, IL-6 and IL-12p70 were measured by RT-qPCR ($n=6$). (**B**) Exudates were collected at 12 h and levels of iNOS in macrophages were measured by flow cytometry. (**C**) Levels of TNF-α in macrophages were measured by flow cytometry at 6 and 12 h. (**D**) Peritoneal macrophages from *Dicer1-C* or *Dicer1-CKO* mice were incubated with pHrodor-labeled Dextran for 30–60 min in vitro and then assessed for phagocytosis by flow cytometry ($n=6$). (**E**) The colony forming units (CFU) after co-culture of different bacteria (including 1×10^6 *S. aureus*, 5×10^7 *E. coli* and 1×10^6 *L. monocytogenes*) and 2×10^6 RAW264.7 macrophages treated with Dicer-siRNA or scramble-siRNA were counted ($n=6$). Error bars represent SEM. Statistical analysis for Fig. 4D was performed via two-way *ANOVA* with Tukey's post-hoc test for multiple comparisons, unpaired two-tailed Student's *t* test was used for the rest comparison. *$p<0.05$; **$p<0.01$; ***$p<0.001$; ****$p<0.0001$

of macrophages expressed the IFN-γ receptor (Fig. 6B), accounting for 60% of all IFN-γ receptor positive cells (Supplementary Fig. 6A). Treatment of mice with anti-IFN-γ antibody prior to inducing peritonitis resulted in a significant restoration of *dicer* mRNA expression compared to the control group at 24 h (Fig. 6C). In vitro experiments further supported these findings, showing that blocking IFN-γ function completely restored *dicer* mRNA expression in BMDM, consistent with the in vivo results (Fig. 6D).

To determine the source of IFN-γ, sector graphs were generated to show the proportion of different types of IFN-γ⁺ cells based on flow cytometry results obtained in vivo. The results indicated that over 80% of IFN-γ⁺ cells were neutrophils (Ly6G⁺ cells) at 6 and 12 h (Fig. 6E and

Supplementary Fig. 6B). Furthermore, it was confirmed that IFN-γ produced by neutrophils could be induced by Zym A in vitro (Fig. 6F), suggesting that Dicer expression in macrophages was primarily influenced by neutrophils during peritonitis progression. To validate the role of neutrophils, an experiment using anti-Ly6G antibody was conducted (Supplementary Fig. 6C), which specifically removed Ly6G⁺ cells in vivo and supported the origin of IFN-γ. The use of anti-Ly6G antibody effectively reduced IFN-γ production, leading to a restoration of Dicer expression at 12 and 24 h (Fig. 6G-H). These findings highlight the significant contribution of IFN-γ derived from neutrophils in suppressing Dicer in macrophages during peritonitis development.
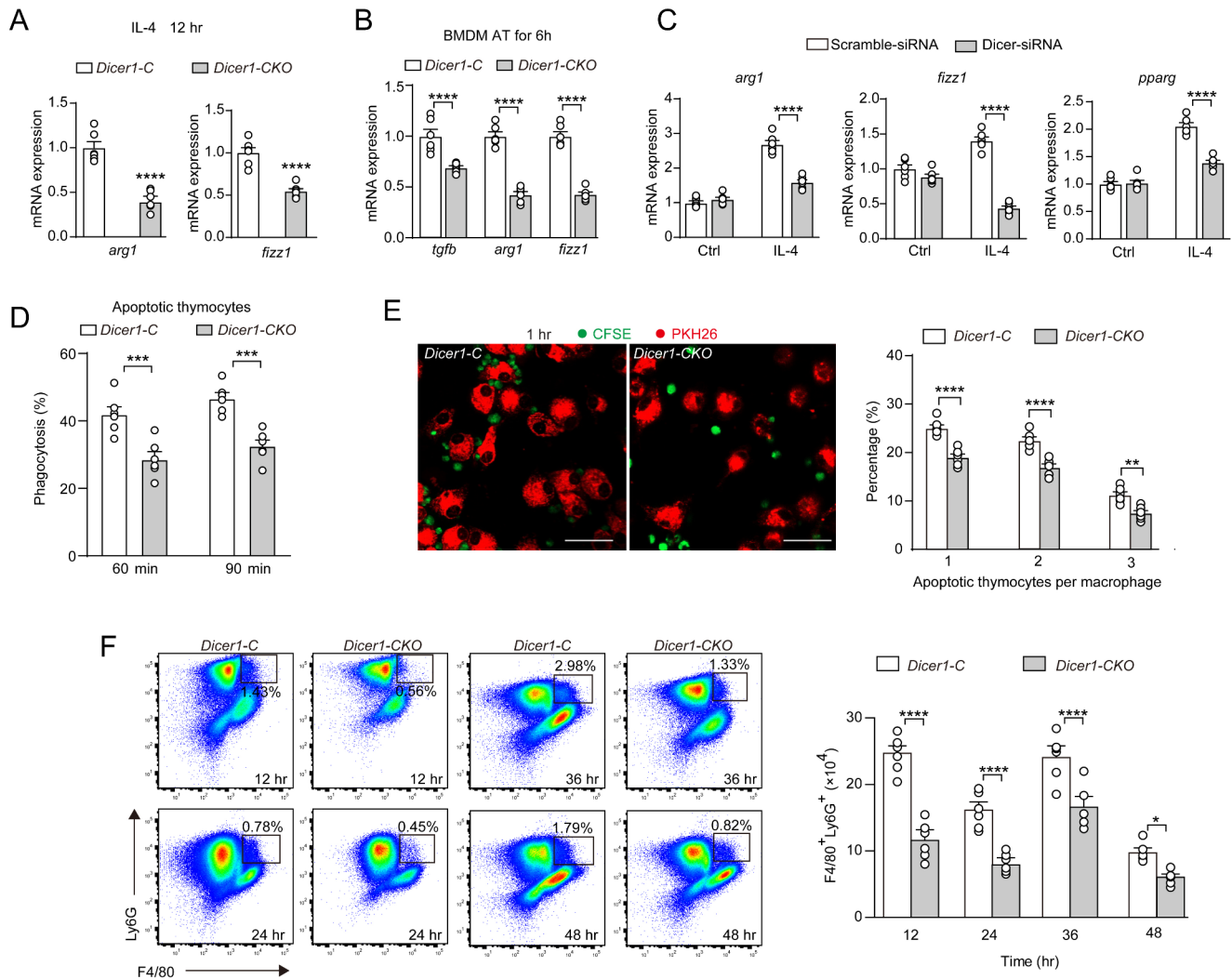
Fig. 5 Dicer deletion inhibits macrophage polarization towards M2 phenotype and impairs macrophage efferocytosis. (**A**) The expression of *arg1* and *fizz1* were detected by RT-qPCR after WT-BMDM or KO-BMDM treated with IL-4 for 12 h (*n*=6). (**B**) The expression level of *tgfb*, *arg1*, and *fizz1* were detected by RT-qPCR after WT-BMDM or KO-BMDM co-cultured with apoptotic thymocytes (*n*=6). (**C**) The expression of *arg1*, *fizz1* and *pparg* were detected by RT-qPCR after Dicer-siRNA or scramble-siRNA-treated RAW264.7 macrophages incubated with IL-4 for 12 h (*n*=6). (**D**) Peritoneal macrophages from *Dicer1-C* or *Dicer1-CKO* mice were incubated with CFSE-labeled apoptotic thymocytes for 60–90 min in vitro and assessed for effe-rocytosis by flow cytometry (*n*=6). (**E**) The engulfment of apoptotic thymocytes (CFSE, green) were measured by laser-scanning confocal microscopy (*n*=6). Peritoneal macrophages were labeled with PKH26 (Red). (**F**) Analysis of in vivo phagocytosis of apoptotic neutrophils by peritoneal macrophages (Ly6G$^+$F4/80$^+$) at 12, 24, 36, and 48 h during Zym A-induced peritonitis by flow cytometry (*n*=6). Error bars represent SEM. Statistical analysis for Fig. 5A was performed via unpaired two-tailed Student's *t* test, two-way *ANOVA* with Tukey's post-hoc test for multiple comparisons was used for the rest analysis. *$p<0.05$; **$p<0.01$; ***$p<0.001$; ****$p<0.0001$

We further investigated the mechanism behind the restoration of Dicer expression during peritonitis resolution. To determine if apoptotic cells play a role in this process, we analyzed *dicer* mRNA expression in peritoneal macrophages (PM) or BMDM co-cultured with apoptotic thymocytes (AT), apoptotic neutrophils (AN), or apoptotic Jurkat cells (AJ) in vitro. Our findings showed a significant up-regulation of *dicer* mRNA expression in both PM and BMDM upon exposure to apoptotic cells (Fig. 7A-D). Interestingly, co-culturing PM with apoptotic cell conditioned medium (ATCM) did not result in any change in *dicer* mRNA expression (Fig. 7E). Furthermore, when we used cytochalasin D (CytD) to inhibit phagocytosis, we observed that the inhibition led to a lack of increase in *dicer* expression (Fig. 7F). In a separate experiment, we injected either PBS or AT into the peritoneal cavity of mice and found a significant increase in *dicer* expression in macrophages in the AT group after 24 h (Fig. 7G). Moreover, intravenous injection of apoptotic thymocytes resulted in increased *dicer* expression in splenic cells after 24 h (Fig. 7H). These results collectively
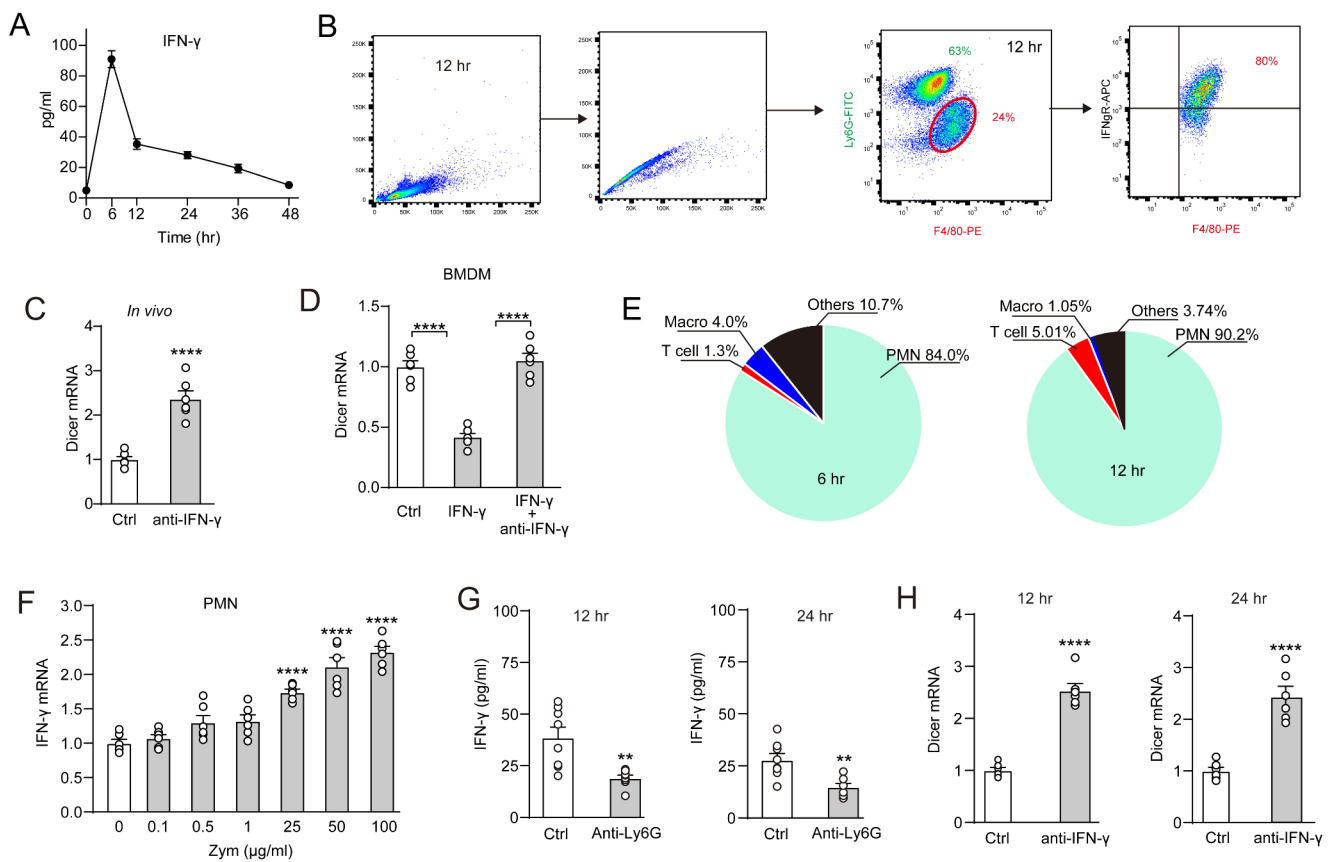
Fig. 6 Neutrophil-derived IFN-γ inhibits Dicer expression in macrophages during the progression of peritonitis WT mice were intraperitoneally injected with 1 mg Zym A to establish acute inflammation. (**A**) The expression level of IFN-γ in the peritoneal exudate during peritonitis were measured by ELISA ($n=6$). (**B**) Cellular distribution of IFN-γR were measured at 12 h by flow cytometry ($n=3$). (**C**) WT mice were intraperitoneally injected with 2 ml anti-IFN-γ antibody (25 ug/ml, clone: XMG1.2, Sungene Biotech) or isotype control antibody (25 ug/ml, Rat IgG1; Sungene Biotech) 24 h before induction of peritonitis by *i.p.* administration with 1 mg Zym A. The expression of Dicer mRNA in peritoneal macrophages at 24 h was measured by RT-qPCR ($n=6$). (**D**) In vitro cultured WT-BMDM were treated with PBS, IFN-γ, or IFN-γ+anti-IFN-γ antibody, mRNA expression of Dicer in BMDM was measured by RT-qPCR ($n=6$). (**E**) WT mice were intraperitoneally injected with 1 mg Zym A to establish acute inflammation,

the cellular proportion of peritoneal IFN-γ⁺ cells were measured by flow cytometry at 6 and 12 h. (**F**) In vitro cultured neutrophils from WT mice were stimulated with different doses of Zym A, mRNA expression of IFN-γ was measured by RT-qPCR ($n=6$). (**G**) WT mice were treated with anti-Ly6G antibody (25 ug/ml, clone: RB6-8C5, Sungene Biotech) or isotype antibody (25 ug/ml, Rat IgG1; Sungene Biotech) 24 h before peritonitis induced by Zym A. The expression level of IFN-γ in peritoneal effusion at 6 and 12 h in vivo was detected by ELISA ($n=8$). (**H**) The mRNA expression of Dicer in peritoneal macrophages at 6 and 12 h were measured by RT-qPCR ($n=6$). Error bars represent SEM. Statistical analysis was performed via unpaired two-tailed Student's t test (C, G and H) or one-way *ANOVA* with Tukey's post-hoc test for multiple comparisons (D, F). *$p<0.05$; **$p<0.01$; ***$p<0.001$; ****$p<0.0001$

indicate that the activation of Dicer expression is linked to the phagocytosis of apoptotic cells, leading to enhanced efferocytosis, rather than being mediated by specific molecules released by apoptotic cells.

Discussion

This study highlights the central role of Dicer in regulating the progression and resolution of innate immune-mediated inflammation (Fig. 8). A novel mechanism for regulating Dicer expression is identified, with a focus on the interactions between neutrophils and macrophages. Experimental

results demonstrate a biphasic modulation of Dicer expression in macrophages during inflammation, influenced by neutrophil-derived IFN-γ and efferocytosis of apoptotic cells. *Dicer1-CKO* mice showed intensified inflammation progression and delayed resolution of peritonitis, emphasizing the importance of Dicer in this process. Additionally, Dicer deletion in macrophages led to M1 polarization and disrupted the transition to the M2 phenotype.

Zym A-induced acute peritonitis displays time-dependent characteristics of leukocyte infiltration during inflammation, involving the migration and aggregation of immune cells like neutrophils and macrophages [24]. This condition initiates local and systemic inflammatory responses, marked
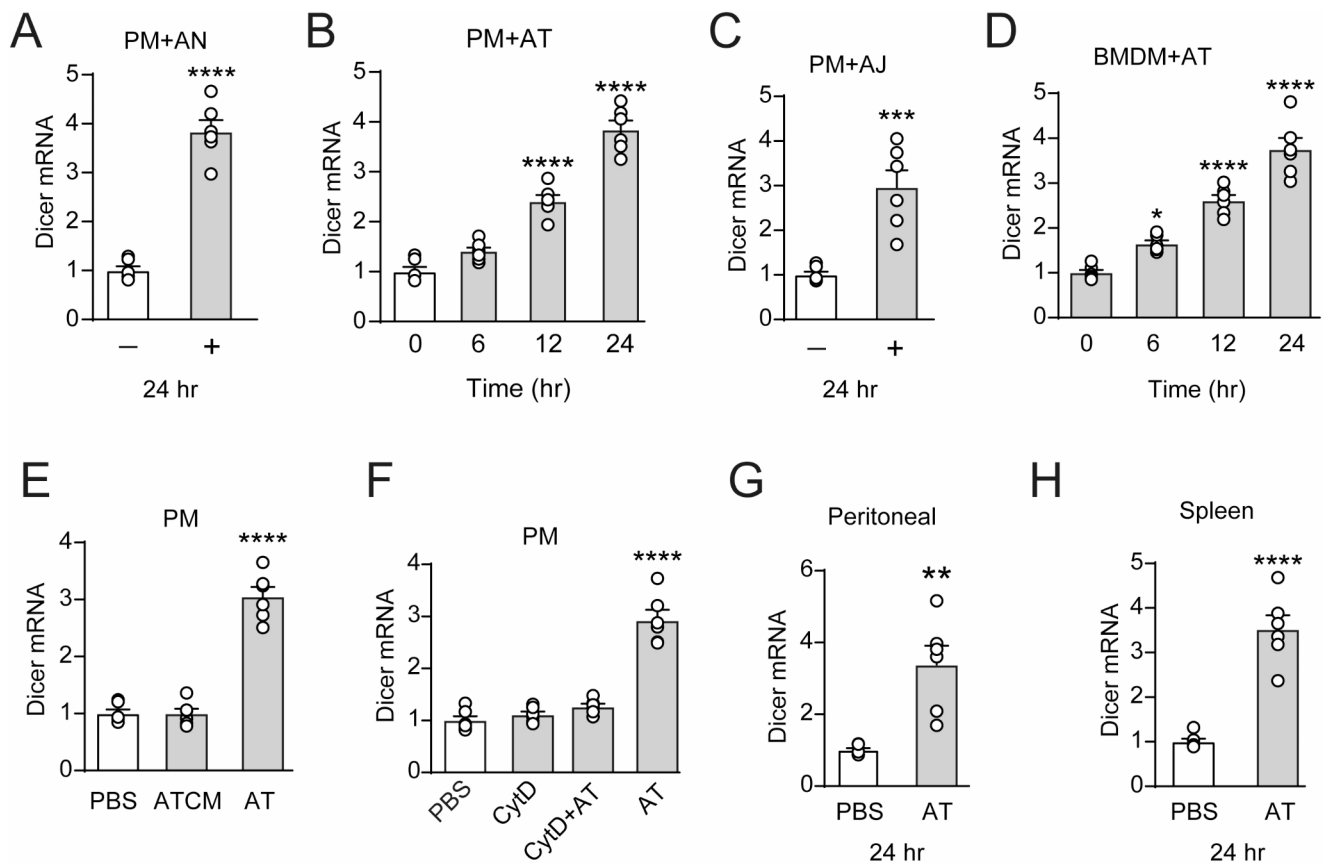
Fig. 7 Efferocytosis of apoptotic cells regulates Dicer expression in macrophages during resolution of inflammation. In vitro cultured peritoneal macrophages (PM) from WT mice were co-incubated with apoptotic neutrophils (**A**), apoptotic thymocytes (**B**) or apoptotic Jurkat cells (**C**) for different times, expression of macrophage Dicer mRNA was measured by RT-qPCR ($n=6$). (**D**) In vitro cultured BMDMs from WT mice were co-incubated with apoptotic thymocytes, Dicer mRNA expression was measured by RT-qPCR ($n=6$). (**E**) Peritoneal macrophages from WT mice were co-cultured with PBS, apoptosis cell conditioned medium, or apoptotic thymocytes for 24 h. Dicer mRNA expression of peritoneal macrophages were measured by RT-qPCR ($n=6$). (**F**) Peritoneal macrophages from WT mice were co-cultured with PBS, 1 ug/ml cytochalasin D (Abcam, ab143484, China), apop-

totic thymocytes, or cytochalasin D together with apoptotic thymocytes for 24 h. Dicer mRNA expression of peritoneal macrophages were measured by RT-qPCR ($n=6$). (**G**) WT mice were intraperitoneally injected PBS or apoptotic thymocytes. After 24 h, the mRNA expression of Dicer in peritoneal macrophages was measured by RT-qPCR ($n=6$). (**H**) WT mice were intravenously injected with PBS or apoptotic thymocytes. Dicer mRNA expression in splenic cells were measured by RT-qPCR ($n=6$) after 24 h. Error bars represent SEM. Statistical analysis was performed via unpaired two-tailed Student's t test (A, C, G, H) or one-way *ANOVA* with Tukey's post-hoc test for multiple comparisons (B, D, E, F). $*p<0.05$; $**p<0.01$; $***p<0.001$; $****p<0.0001$

by the release of inflammatory mediators, vasodilation, and exudate formation, typical signs of inflammation. These features diminish rapidly over time, eventually restoring normal physiological conditions in the organism. Numerous studies have highlighted the critical role of Dicer in maintaining inflammatory balance [25]. Our recent research indicates that Dicer expression is dynamically regulated during acute peritonitis, closely linked to the progression and resolution of inflammation. Specifically, we observed downregulation of Dicer during inflammation progression, followed by a return to near-normal levels during the resolution phase, suggesting a pivotal role for Dicer in regulating the inflammatory process.

During acute peritonitis, macrophages and neutrophils play key roles in the inflammatory response by releasing cytokines and chemical mediators that regulate inflammation. Previous research has extensively documented the interaction between neutrophils and macrophages, showing that neutrophils can influence macrophage polarization through cytokines and cell-cell interactions [14]. Our study has discovered a new pathway where neutrophils secrete IFN-γ to drive macrophage differentiation towards the M1 phenotype in a self-limited inflammation model, enhancing their ability to combat bacteria and respond quickly to inflammation. Additionally, cell-cell interactions between neutrophils and macrophages, mediated by receptors and ligands, also impact macrophage polarization. For example,
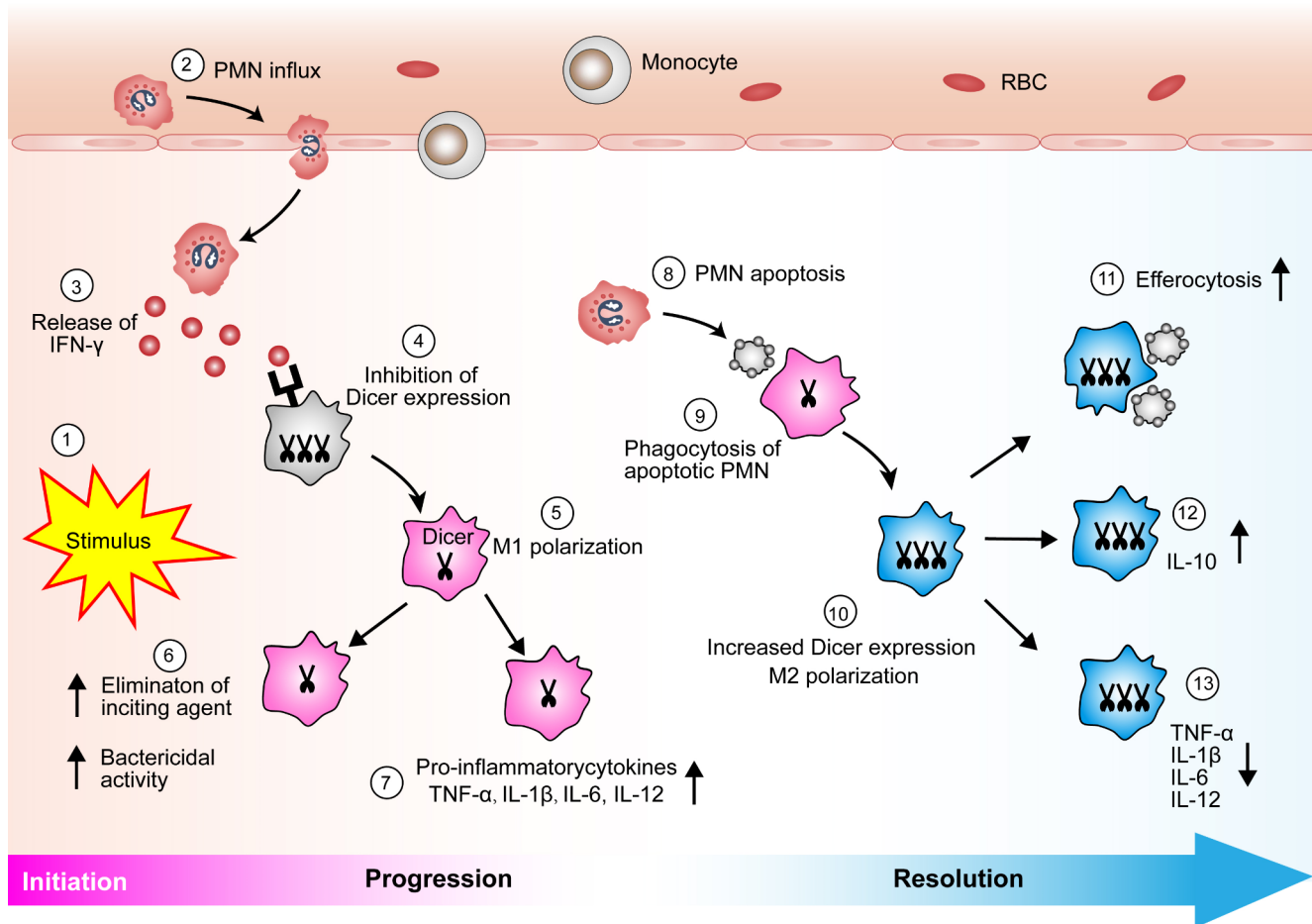
Fig. 8 Dynamic regulation of macrophage Dicer by neutrophils play a central role in the progression and resolution of acute inflammation. Following inflammatory stimulus (1), neutrophils are recruited to the site of inflammation (2), activated neutrophils release pro-inflammatory cytokine IFN-γ (3), binding to IFN-γ receptors which are mainly expressed on macrophages, leads to inhibition of Dicer expression in macrophages (4). Down-regulation of Dicer induces a M1 polarization (5), which leads to increased phagocytosis and bactericidal functions (6), and produce pro-inflammatory cytokines such as TNF-α, IL-1β, IL-6 and IL-12 (7), therefore promotes the pro-inflammatory progression phase of inflammation; During the resolution phase, apoptosis of PMNs occurs (8) and efferocytosis of apoptotic neutrophils by macrophages (9) restores the expression of Dicer, resulting in a switch from M1 to M2 polarization in macrophages (10). M2 macrophages exhibit higher ability of efferocytosis (11), increased level of anti-inflammatory IL-10 (12), and lower levels of pro-inflammatory TNF-α, IL-1β, IL-6 and IL-12 (13), therefore accelerating the resolution of inflammation

molecules on the surface of neutrophils like ICAM-1 and PECAM-1 can bind with macrophage ligands, influencing macrophage polarization [26, 27]. Our research further shows that the phagocytosis of apoptotic neutrophils by macrophages promotes the differentiation of macrophages into M2 macrophages, aiding in the resolution of inflammation.

Current studies have shown that Dicer plays a role in processing precursor miRNAs (pre-miRNAs) into mature miRNAs, which are short non-coding RNAs that regulate gene expression by interacting with target mRNAs to either inhibit translation or promote mRNA degradation [28]. In macrophages, specific miRNAs processed by Dicer can target key signaling pathways or transcription factors involved in macrophage polarization, influencing their phenotype and functional properties [29–31]. For instance, miRNAs

can modulate the balance between pro-inflammatory M1 macrophages and anti-inflammatory M2 macrophages, thereby shaping the immune response to infection, tissue damage and resolution of inflammation [31–33]. Our analysis revealed that the expression of Dicer is dynamically regulated in self-limited peritonitis, with decreased expression during the initiation/progression phase and restoration to near-normal levels during the resolution phase. This regulation is crucial for maintaining inflammation homeostasis, as evidenced by severe inflammation progression and delayed resolution in Dicer-knockout mice. Additionally, we observed that IFN-γ plays a role in inhibiting Dicer expression during the progression phase, promoting macrophage differentiation towards the M1 phenotype. This observation aligns with the findings of Caroline Baer et

al., who demonstrated that conditional deletion of Dicer in macrophages leads to the development of M1-like tumor-associated macrophages (TAMs) due to hyperactive IFN-γ/STAT1 signaling [20]. Conversely, another study indicated that restoring Dicer expression in inflamed colon tissues can alleviate colitis and prevent colitis-associated tumorigenesis [34]. In our study, we found that increased Dicer expression in macrophages following the clearance of apoptotic cells promoted M2 polarization and aided in the resolution of inflammation.

Increasing literatures reveal that miRNA plays a pivotal role in shaping the resolution phase of inflammation [33, 35]. For example, miR-466 L overexpression in macrophages increased special proresolving mediators (SPMs) such as resolvin D1 [RvD1] and RvD5 which enhanced resolution of inflammation [36]. Elevated miR-21 in macrophage promotes efferocytosis, an important component of the resolution phase, by inducing M1 to M2 macrophage phenotype switch [37]. Our studies on self-limiting peritonitis in Dicer-CKO mice provide a broader perspective supporting the involvement of miRNAs in the resolution of inflammation. In addition to peritonitis model, the role of Dicer-regulated miRNAs in inflammation across different organs and tissues has been reported. In atherosclerosis, Dicer/miR-10a plays an atheroprotective role by coordinately regulating the inflammatory response and lipid metabolism in macrophages [38]. In the nervous system, Dicer-deficient microglia expressed more pro-in flammatory cytokines than wild-type microglia after peripheral LPS exposure, indicating that Dicer-controled miRNAs were required to limit microglial responses to challenge [39]. These findings emphasize the essential role of Dicer in regulating inflammatory response across various organs and tissues through its influence on miRNAs. Although current studies have not provided direct evidence that macrophage Dicer is involved in the regulation of inflammation in sepsis models, numerous findings have highlighted the critical role of miRNAs in this process [31, 40]. For instance, in septic mice via cecal ligation and puncture (CLP), induction of miR-146a expression in splenic macrophages prevents excessive inflammation and multiple organ injury [41]. In another sub-acute sepsis model, miR-223 control the progress of sepsis by modulating M2 polarization of macrophages [42]. Therefore, it is possible that information from Dicer-regulated M2 polarization and inflammation resolution can be translated to treat sepsis. LysM-Cre$^{+/+}$ murine model is known to effect gene deletion in both macrophages and neutrophils [43]. Although our data demonstrating that the ablation of Dicer in neutrophils did not markedly affect oxidative stress, apoptosis, or mitochondrial membrane potential, the precise role of neutrophil-specific Dicer in the initiation and resolution of inflammation remains elusive.

Consequently, the utilization of macrophage-specific Cre driver mice such as Cx3cr1-Cre murine model, is deemed essential infurther studies to elucidate the distinct contributions of Dicer within macrophages and neutrophils.

In summary, our results demonstrate that the modulation of Dicer expression in macrophages by neutrophil-derived IFN-γ and efferocytosis of apoptotic cells plays a crucial role in the regulation of acute inflammation. This study, in line with existing research, highlights a unique macrophage-specific function of Dicer in inflammation modulation through M1/M2 polarization control. However, therapeutic interventions targeting Dicer present a complex scenario that requires precise timing and approach. Furthermore, our current knowledge of the intricate regulatory mechanisms governing Dicer gene expression remains limited. Therefore, a deeper exploration of these pathways could offer valuable insights and potential therapeutic targets for inflammatory disease treatment.

Materials and methods

Animals

All mice were bred in a pathogen-free environment at the animal facility of Army Medical University. Mice referred to as *Dicer1-C* and *Dicer1-CKO* were either LysM-Cre$^{-/-}$/Dicer1$^{loxp/loxp}$ or LysM-Cre$^{+/+}$/Dicer1$^{loxp/loxp}$. For all experiments, mice aged between 10 and 12 weeks were selected and matched based on age and sex.

Zym A-induced peritonitis and treatment

Mice were anesthetized with 4% isoflurane and peritonitis was induced by intraperitoneal (*i.p.*) administration of 1 mg/mouse Zym A (Sigma-Aldrich, St Louis, MO, USA) in 1 ml of sterile PBS.For the analysis, six mice from each group were examined at 6, 12, 24, 36, and 48 h after Zym A administration, with additional analysis of mice not injected with Zym A (0 h). Sampling was done under deep isoflurane anesthesia, and peritoneal exudates were collected immediately by lavage with 5 ml of ice-cold sterile PBS. The cells were filtered through a 70 μm cell strainer (BD Biosciences, Franklin Lakes, NJ, USA) and then centrifuged at 300 g for 10 min at 4 °C. The cells were incubated in 5 ml of RBC lysis buffer (eBioscience, San Diego, CA, USA) for 5 min at room temperature. The collected leukocytes were used for protein extraction or flow cytometry analysis. To determine the exudate cell composition, the total number of infiltrated leukocytes was counted using trypan blue. Neutrophils (Ly6G$^+$CD11$^+$) and monocytes/macrophages (Ly6G$^-$CD11b$^+$) were identified by staining the lavage cells

with anti-mouse Ly6G (1:100, Sungene Biotech, Tianjin, China) and anti-mouse CD11b antibodies (1:100, Sungene Biotech, Tianjin, China) and then analyzed by flow cytometry. Peritoneal exudates were collected at specified intervals for the experiments.

The resolution of acute inflammation was assessed using the following resolution indices: Ψ_{max}, representing the peak neutrophil numbers; T_{max}, indicating the time of peak neutrophil infiltration; Ψ_{50}, denoting 50% of the maximum neutrophil count; T_{50}, representing the time when neutrophil numbers decrease to 50% of the maximum; R_i (resolution interval, T_{50}-T_{max}), indicating the time period during which 50% of neutrophils are lost from exudates.

Wound-healing model

Initially, full-thickness skin (including the panniculus carnosus) wounds of equal area were created in both *Dicer1-C* and *Dicer1-CKO* groups under sterile conditions. Briefly, mice were anesthetized by *i.p.* with pentobarbital sodium (50 mg/kg; Boster, Wuhan, China). After depilation with 8% Na_2S and cleaning with povidoneiodine and 75% ethanol, the dorsal skin was picked up at the midline and punched with a sterile disposable biopsy punch (6 mm in diameter; Miltex, New York, NY, USA), generating two wounds on each side of the midline. At indicated time points, each wound was digitally photographed, and wound areas were quantified using CorelDRAW 9 (Corel Software, Oakland, CA, USA). Changes in wound areas over time were expressed as the percentage of initial (day 0) wound area.

In vitro phagocytosis assay

An in vitro phagocytosis assay was conducted using mouse peritoneal macrophages following established procedures with slight modifications. Briefly, wild type C57BL/6 mice aged 10–12 weeks were intraperitoneally injected with 3% Brewer's thioglycollate (Sigma-Aldrich, St Louis, MO, USA). After 72 h, primary peritoneal macrophages were retrieved from peritonitis exudates through peritoneal lavage using 5 ml of ice-cold DMEM twice. The macrophages were then cultured in Φ20mm Glass Bottom Cell Culture Dishes in DMEM with 10% FCS and allowed to rest overnight at 37 °C in 5% CO2 before commencing experiments.

To assess macrophage phagocytosis of apoptotic thymocytes in vitro, we labeled apoptotic thymocytes with CFSE (Green) and peritoneal macrophages with PKH26 (Red). The CFSE-labeled apoptotic thymocytes were then incubated with macrophages at a 1:5 ratio and cultured at either 4 °C (negative control) or 37 °C for 60, 90, or 120 min in RPMI 1640 supplemented with 10% FBS. After washing off

the free cells, phagocytosis was visualized using laser confocal microscopy.

To assess macrophage phagocytosis of Zym A and dextran beads in vitro, peritoneal macrophages were treated with pHrodo-labeled Zym A (Molecular Probes, Eugene, Oregon, USA) at a 1:10 ratio for 60 min or with 0.5 mg/ml FITC-dextran (molecular weight 40,000; Sigma-Aldrich, St Louis, MO, USA) for 30 min at room temperature. Subsequently, macrophages were harvested, stained with anti-mouse CD11b antibody (1:100, Sungene Biotech, Tianjin, China) and anti-mouse F4/80 antibody (1:100, Sungene Biotech, Tianjin, China), and the proportion of $CD11b^+F4/80^+pHrodo^+$ or $CD11b^+F4/80^+FITC^+$ macrophages to $CD11b^+F4/80^+$ macrophages was determined using flow cytometry.

In vivo phagocytosis assay

In in vivo splenic macrophage uptake assays, 8×10^7 pHrodo-labeled apoptotic thymocytes were intravenously injected into 10- to 12-week-old mice. Two hours after the injection of apoptotic thymocytes, the mice were sacrificed, and their spleens were collected. Splenocytes were obtained by grinding with a 70-μm cell strainer. Single splenocyte suspensions were processed similarly to peritoneal lavage fluid, and the cells were then analyzed by flow cytometry to quantify the number of spleen macrophages engulfing pHrodo-labeled apoptotic thymocytes.

Flow cytometry

Single-cell suspensions were prepared from cultured cells and peritoneal lavage of mice. The cells were washed twice in staining buffer, resuspended, and treated with anti-CD16/32 antibodies (0.5 μg/million cells, Sungene Biotech, Tianjin, China) to block Fc receptors. Subsequently, surface antibody staining was performed with labeled antibodies diluted in staining buffer for 20 min at 4 °C. After incubation, the cells were washed and immediately analyzed. For intracellular staining of TNF-α and iNOS, samples were fixed and permeabilized using Intracellular Fixation & Permeabilization Buffer (eBioscience, San Diego, CA, USA) after surface staining, followed by incubation with TNF-α (1:100, Abcam, Cambridge, UK) or iNOS antibodies (1:100, Abcam, Cambridge, UK). Isotype controls were used for all staining. Post surface and intracellular staining, cells were washed, suspended in PBS, and analyzed using CANTO II (Becton Dickinson, Franklin Lakes, NJ, USA). Labeled antibodies including CD11b (1:100, Sungene Biotech, Tianjin, China), F4/80 (1:100, Sungene Biotech, Tianjin, China), and Ly6G (1:100, Sungene Biotech, Tianjin, China) were employed to identify various leukocyte subpopulations.

To determine neutrophil apoptosis in vivo, exudate cells were labeled with annexin-V (1:20, Sungene Biotech, Tianjin, China) and Ly-6G antibody (1:100, Sungene Biotech, Tianjin, China). The population of annexin-V$^+$Ly6G$^+$ neutrophils was assessed using flow cytometry. Flow data were acquired using CellQuest Software and analyzed with FlowJo software for Windows (Treestar, Inc.).

Blockade of IFN-γ and Ly6G

To block IFN-γ in vivo, mice received a single 2 ml dose of rat anti-IFN-γ monoclonal antibody (25 ug/ml, clone: XMG1.2, Sungene Biotech) or isotype control antibody (25 ug/ml, Rat IgG1; Sungene Biotech) *via* intraperitoneal (*i.p.*) administration 24 h prior to intraperitoneal administration of 1 mg/mouse Zym A. Similarly, for in vivo Ly6G blockade, mice were administered a 2 ml dose of rat anti-Ly6G monoclonal antibody (25 ug/ml, clone: RB6-8C5, Sungene Biotech) or isotype control antibody (25 ug/ml, clone: Rat IgG2b; Sungene Biotech) *via i.p.* administration 24 h before Zym A administration. To block IFN-γ in vitro, the XMG1.2 antibody (5 ug/ml) was incubated with IFN-γ (5 ng/ml) in 1 ml sterile PBS at 37 °C for 2 h. Subsequently, 10^6 BMDM were added to the mixture of XMG1.2 antibody and IFN-γ and incubated for 12 h before cell collection for RT-qPCR.

Western blotting

For Western blot analysis, macrophages (Ly6G$^-$CD11b$^+$ F4/80$^+$) were isolated from the peritoneal exudate by flow cytometry sorter and homogenized in ice-cold RIPA buffer with 1 mg/mL of a protease inhibitor cocktail (Beyotime Institute of Biotechnology, Haimen, China). The homogenates were centrifuged at 12,500 rpm for 5 min at 4 °C and the supernatants were collected. BCA assays were subsequently performed to normalize protein levels, and cell extracts were applied to 10% sodium dodecyl sulfate polyacrylamide gel electrophoresis, transferred onto polyvinylidene difluoride membrane, blocked in 5% non-fat milk in TBST (0.9% NaCl and 0.05% Tween-20 in 20 mM Tris/HCl, pH 7.4) for 1 h, and incubated with following antibodies: Dicer (1:1000, AF6702, Beyotime, Haimen, China), GAPDH (1:1000, AB-P-R001, Goodhere Biotechnology, Hangzhou, China) for 1 h followed by addition of secondary antibody the goat anti-rabbit IgG-HRP secondary antibody (1:1000, NBP1-75297, Novus Biologicals, Littleton, CO, USA) for 30 min. Blots were washed and detection was performed using an enhanced chemiluminescence system BeyoECL Plus (Beyotime, Haimen, China). All conditions were expressed as a ratio of test protein to GAPDH. Experiments are representative of at least 3 independent experiments.

Bone marrow-derived macrophages (BMDM)

To generate bone marrow-derived macrophages (BMDM), bone marrow cells were obtained by flushing femurs and tibias from *Dicer1-C* or *Dicer1-CKO* mice with a sterile saline solution. The isolated cells were plated in 10 cm Petri dishes at 1×10^6 cells/mL in Dulbecco's modified Eagle's media (DMEM), supplemented with 10% heat-inactivated fetal bovine serum (FBS), 1% penicillin/streptomycin, 1% glutamine, and 20 ng/mL of macrophage colony-stimulating factor (M-CSF, BioLegend). On day 7, the macrophages were harvested, washed, counted, and replated in culture media (without M-CSF) at a density of 2×10^6 cells/well.

Isolation and function assay of murine neutrophils

Bone marrow derived neutrophils were isolated by Percoll gradients, as described previously. Mice were euthanized, and bone marrow was removed from the femurs by perfusion of 6 mL of cold PBS. Bone marrow cells were pelleted by centrifugation and resuspended in 2 mL of PBS. Percoll solutions were prepared by mixing Percoll solution and $10 \times$ PBS at a 1:9 ratio to obtain a 100% Percoll stock, which was diluted with PBS for gradients of 72%, 60%, and 52%. Prior to centrifugation (1100 g, 30 min), marrow cell suspensions were loaded in the uppermost layer. The neutrophils were collected in the band between the 72% and 60% layers.

For ROS and hypoxia assay, the neutrophils were recovered by centrifugation at 300 g for 5 minutes, resuspended in 200 μL of Hypoxia/Oxidative Stress Detection Mix (5×10^5 cells/sample) and then incubated under normal tissue culture conditions for 0.5 h. Samples were washed and analyzed using flow cytometry according to product manual (Cyto-ID Hypoxia/Oxidative Stress Detection Kit, Enzo Life Sciences, ENZ-51042, Farmingdale, NY, USA).

For apoptosis assay, neutrophils were fixed and permeabilized by Intracellular Fixation & Permeabilization Buffer Set (eBioscience, 88-8824-00, USA). Then samples were stained with anti-Caspase-3 antibody (Abcam, ab32351, China) and assayed by flow cytometry.

For investigate the mitochondrial membrane potential, suspension neutrophils in PBS were incubate with JC solution (JC1- Mitochondrial Membrane Potential Assay Kit, Abcam, ab113850, China) for 30 min at 37ºC and assayed by flow cytometry.

Real-time quantitative PCR

RNA was extracted from cultured macrophages using the RNA fast 200 Kit (Fastagen, Shanghai, China) following the manufacturer's instructions. Subsequently, reverse transcription was carried out with a kit from Takara (Tokyo,

Japan). Quantitative polymerase chain reaction (qPCR) was performed using SYBR Green qPCR Master Mix (Med-ChemExpress, Monmouth Junction, NJ, USA) and run on the CFX96 detection system (Bio-Rad Laboratories, Hemel Hempstead, UK). The gene expression levels were reported as the relative mRNA level (fold change) compared to the controls, with their expression levels normalized to 1. The RT-qPCR assay utilized the following primers: *dicer* (forward, 5′-GCA GGC TTT TAC ACA CGC CT-3′; 5′-GGG TCT TCA TAA AGG TGC TT-3′), *inos* (forward, 5′-CAG CTG GGC TGT ACA AAC CTT-3′; 5′-CAT TGG AAG TGA AGC GTT TCG-3′), *tnfa* (forward, 5′-AAC TAG TGG TGC CAG CCG AT-3′; 5′-CTT CAC AGA GCA ATG ACT CC-3′), *tgfb* (forward, 5′-CCA CCT GCA AGA CCA TCG AC-3′; reverse, 5′-CTG GCG AGC CTT AGT TTG GAC-3′), *mcp1* (forward, 5′-AGC CAA CTC TCA CTG AAG CC-3′, reverse, 5′-TCT CCA GCC TAC TCA TTG GGA-3′), *il1b* (forward, 5′-GAA ATG CCA CCT TTT GAC AG-3′; 5′-TGG ATG CTC TCA TCA GGA CAG-3′), *il6* (forward, 5′-TGA TGG ATG CTA CCA AAC TGG-3′; 5′-TGG TCT TGG TCC TTA GCC ACT-3′), *il12p70* (forward, 5′-TGA ACT GGC GTT GGA AG-3′; 5′-GAA GTA GGA ATG GGG AGT G-3′), *arg1* (forward, 5′-AAG CTG GTC TGC TGG AAA AA-3′; 5′-CTG GTT GTC AGG GGA GTG TT-3′), *fizz1* (forward, 5′-TCC CAG TGA ATA CTG ATG AGA-3′; 5′-CCA CTC TGG ATC TCC CAA GA-3′), *ifng* (forward, 5′-GCT GTT ACT GCC ACG GCA CAG T-3′; 5′-CAC CAT CCT TTT GCC AGT TCC TCC-3′), *pparg* (forward, 5′-AGT CCT CAC AGC TGT TTG CCA AGC-3′; 5′-GAG CGG GTG AAG ACT CAT GTC TGT C-3′), *actb* (forward, 5′-TGG AAT CCT GTG GCA TCC ATG AAA-3′; reverse, 5′-TAA AAC GCA GCT CAG TAA CAG TCC G-3′). The expression of each gene was normalized to GAPDH mRNA content and calculated using comparative $2^{-\Delta\Delta Ct}$ methods.

Bacterial strains and growth conditions

E. coli serotype O6: K2: H1 was cultured in Luria-Bertani (LB) medium, whereas *L. monocytogenes* and *S. aureus* ATCC25923 were cultured in brain heart infusion (BHI) broth, both at 37 °C with agitation at 220 rpm. The bacteria were washed twice with PBS prior to inoculation into the mouse peritoneum and quantified by plating for viable colony-forming units (c.f.u.) on LB or BHI agar plates.

Bacterial killing assay

To investigate the bactericidal function of macrophages, RAW264.7 cells (2×10^6) were incubated with *E. coli* (strain ATCC-29522, 5×10^7), *S. aureus* (strain Newman, 1×10^6), or *L. monocytogenes* (1×10^6) for 2 h. Subsequently, the cells were washed with PBS and incubated in DMEM medium

with antibiotics for 24 h before harvesting intracellular bacteria. The cell lysate containing intracellular bacteria was serially diluted with PBS and plated on agar plates to assess bacterial viability.

Antibodies and reagents

The antibodies used were as follows: anti-Ly6G antibody (clone: RB6-8C5, Sungene Biotech, Tianjin, China), anti-IFN-γ antibody (clone: XMG1.2, Sungene Biotech, Tianjin, China), annexin-V (Sungene Biotech, Tianjin, China), IFN-γ (abcam, China), IL-4 (abcam, China).

Statistical analysis

Data from three independent experiments were analyzed using GraphPad Prism 9 and presented as means ± SEM. Statistical analysis was carried out with one-way or two-way *ANOVA* followed by Tukey's post-hoc test for multiple comparisons, or two-tailed unpaired Student's *t*-test for two groups. Statistical significance was denoted by asterisks: one for p-value < 0.05, two for p-value < 0.01, three for p-value < 0.001, and four for p-value < 0.0001.

Declarations

Ethics approval The animal study underwent review and approval by the Administration District Official Committee of Army Medical University, located in Chongqing, China.

Consent for publication All authors gave their consent for publication.

Conflict of interest The authors declare that the research was conducted in the absence of any commercial or financial relationships that could be construed as a potential conflict of interest.

References

1. Medzhitov R (2008) Origin and physiological roles of inflammation. Nature 454(7203):428–435
2. Gilroy DW (2021) Resolving inflammation. Nat Rev Immunol 21(10):621–621
3. Watanabe S et al (2019) The role of macrophages in the resolution of inflammation. J Clin Invest 129(7):2619–2628
4. Serhan CN, Sulciner ML (2023) Resolution medicine in cancer, infection, pain and inflammation: are we on track to address the next pandemic?? Cancer Metastasis Rev 42(1):13–17
5. Sansbury BE, Spite M (2016) Resolution of acute inflammation and the role of resolvins in immunity, thrombosis, and vascular biology. Circul Res 119(1):113–130
6. Kumar KP, Nicholls AJ, Wong CHY (2018) Partners in crime: neutrophils and monocytes/macrophages in inflammation and disease. Cell Tissue Res 371(3):551–565
7. Tardito S et al (2019) Macrophage M1/M2 polarization and rheumatoid arthritis: A systematic review. Autoimmun Rev, 18(11)
8. Chen SZ et al (2023) Macrophages in immunoregulation and therapeutics. Signal Transduct Target Therapy, 8(1)
9. Serhan CN (2014) Pro-resolving lipid mediators are leads for resolution physiology. Nature 510(7503):92–101
10. Zhong X et al (2018) Myc-nick promotes efferocytosis through M2 macrophage polarization during resolution of inflammation. FASEB J 32(10):5312–5325
11. Sica A, Mantovani A (2012) Macrophage plasticity and polarization: in vivo veritas. J Clin Invest 122(3):787–795
12. Werner M et al (2019) Targeting biosynthetic networks of the Proinflammatory and proresolving lipid metabolome. FASEB J 33(5):6140–6153
13. Patel AA, Ginhoux F, Yona S (2021) Monocytes, macrophages, dendritic cells and neutrophils: an update on lifespan kinetics in health and disease. Immunology 163(3):250–261
14. Selders GS et al (2017) An overview of the role of neutrophils in innate immunity, inflammation and host-biomaterial integration. Regen Biomater 4(1):55–68
15. Chen F et al (2014) Neutrophils prime a long-lived effector macrophage phenotype that mediates accelerated helminth expulsion. Nat Immunol 15(10):938–946
16. Schilperoort M et al (2023) The role of efferocytosis-fueled macrophage metabolism in the resolution of inflammation. Immunol Rev 319(1):65–80
17. Chen S et al (2023) Macrophages in immunoregulation and therapeutics. Signal Transduct Target Ther 8(1):207
18. Zapletal D et al (2023) Dicer structure and function: conserved and evolving features. EMBO Rep, 24(7)
19. Wei YY et al (2018) Dicer in macrophages prevents atherosclerosis by promoting mitochondrial oxidative metabolism. Circulation 138(18):2007–2020
20. Baer C et al (2016) Suppression of MicroRNA activity amplifies IFN-γ-induced macrophage activation and promotes anti-tumour immunity. Nat Cell Biol 18(7):790–
21. Luo X et al (2020) Metformin shows anti-inflammatory effects in murine macrophages through Dicer/microribonucleic acid-34a-5p and Microribonucleic acid-125b-5p. J Diabetes Invest 11(1):101–109
22. Cash JL, White GE, Greaves DR (2009) *Zymosan-Induced Peritonitis as a Simple Experimental System for the Study of Inflammation.* Methods in Enzymology, Vol 461: Chemokines, Part B, 461: pp. 379–396
23. Mao QDZ et al (2021) Macrophage Dicer promotes tolerogenic apoptotic cell clearance and immune tolerance by inhibiting Pentose phosphate pathway activity. Cell Mol Immunol 18(7):1841–1843
24. Schwab JM et al (2007) Resolvin E1 and protectin D1 activate inflammation-resolution programmes. Nature 447(7146):869–874
25. Cobb BS et al (2006) A role for Dicer in immune regulation. J Exp Med 203(11):2519–2527
26. Woodfin A, Voisin MB, Nourshargh S (2007) PECAM-1: A multi-functional molecule in inflammation and vascular biology. Arterioscler Thromb Vascular Biology 27(12):2514–2523
27. Paulsen K et al (2015) *Regulation of ICAM-1 in Cells of the Monocyte/Macrophage System in Microgravity.* Biomed Research International, 2015
28. Luo QJ et al (2021) RNA structure probing reveals the structural basis of Dicer binding and cleavage. Nat Commun, 12(1)
29. Ojcius DM et al (2019) Dicer regulates activation of the NLRP3 inflammasome. PLoS ONE, 14(4)
30. De Cauwer' A et al (2018) DICER1: A key player in rheumatoid arthritis, at the crossroads of cellular stress, innate immunity, and chronic inflammation in aging. Frontiers in Immunology, p 9
31. Essandoh K et al (2016) MiRNA-Mediated macrophage polarization and its potential role in the regulation of inflammatory response. Shock 46(2):122–131
32. Nie M et al (2016) MicroRNA-155 facilitates skeletal muscle regeneration by balancing pro- and anti-inflammatory macrophages. Cell Death & Disease, p 7
33. Alam MM, O'Neill LA (2011) MicroRNAs and the resolution phase of inflammation in macrophages. Eur J Immunol 41(9):2482–2485
34. Wu XL et al (2020) Rescuing Dicer expression in inflamed colon tissues alleviates colitis and prevents colitis-associated tumorigenesis. Theranostics 10(13):5749–5762
35. Naqvi RA et al (2022) MicroRNAs in shaping the resolution phase of inflammation. Semin Cell Dev Biol 124:48–62
36. Li Y et al (2013) Plasticity of leukocytic exudates in resolving acute inflammation is regulated by MicroRNA and proresolving mediators. Immunity 39(5):885–898
37. Das A et al (2014) Engulfment of apoptotic cells by macrophages: a role of microRNA-21 in the resolution of wound inflammation. J Immunol 192(3):1120–1129
38. Wei Y et al (2018) Dicer in macrophages prevents atherosclerosis by promoting mitochondrial oxidative metabolism. Circulation 138(18):2007–2020
39. Varol D et al (2017) Dicer deficiency differentially impacts microglia of the developing and adult brain. Immunity 46(6):1030–1044e8
40. Zhou X, Li X, Wu M (2018) MiRNAs reshape immunity and inflammatory responses in bacterial infection. Signal Transduct Target Ther 3:14
41. Funahashi Y et al (2019) miR-146a targeted to Splenic macrophages prevents sepsis-induced multiple organ injury. Lab Invest 99(8):1130–1142

42. Wang X et al (2021) MicroRNA-223 modulates the IL-4-medicated macrophage M2-type polarization to control the progress of sepsis. Int Immunopharmacol 96:107783

43. Clausen BE et al (1999) Conditional gene targeting in macrophages and granulocytes using lysmcre mice. Transgenic Res 8(4):265–277